



Numerical simulation of kinetic interface sensitive tracers in laboratory column experiments with COMSOL Multiphysics

Fengchao Sun¹, Dr. Frieder Maier², Dr. Alexandru Tatomir³, Prof. Martin Sauter³

¹Helmholtz Zentrum München, Institute of Groundwater Ecology, Environmental Isotope Chemistry

²Comsol Multiphysics GmbH

³George August University of Göttingen, Faculty of Geoscience and Geography

Background

What are Kinetic interface sensitive tracers (KIS tracers)? Why is it important?

Objectives

To get a better understanding of KIS tracers development.

Lab Experiment

Column Experiment.

Numerical Modeling

Discretisation effect, boundary effect, sensitivity analysis.

Results

Breakthrough behavior of non-wetting phase and KIS tracer products.

Conclusions

Background

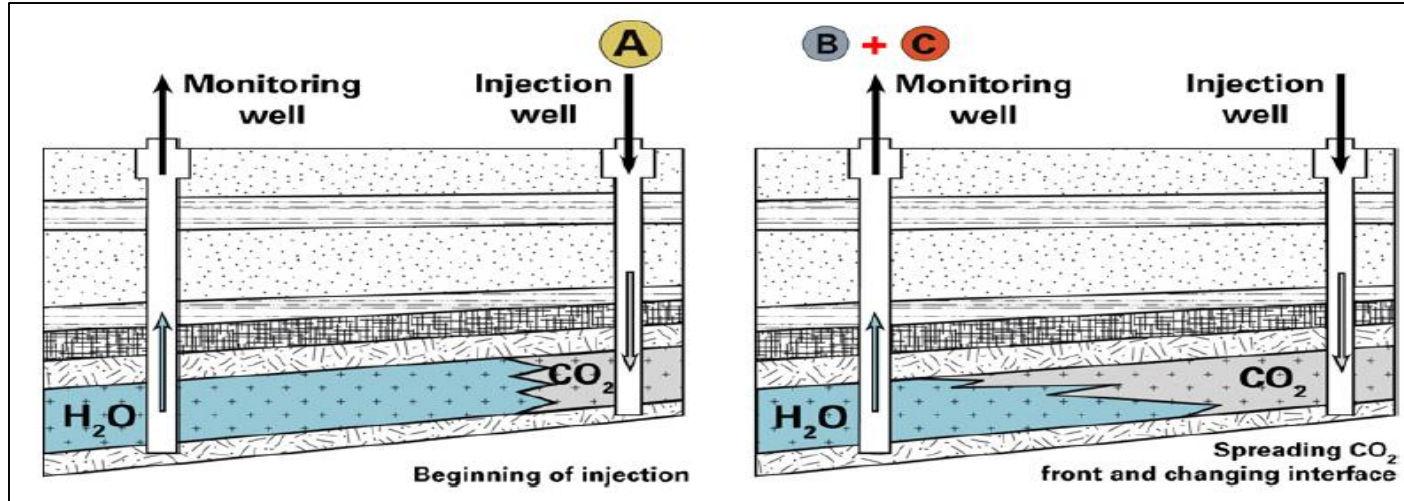


Fig. 1 Injection well: Injection and spreading of scCO₂ together with dissolved KIS tracer. Monitoring well: Measurement of KIS tracer reaction products in the brine, Schaffer et al. 2013

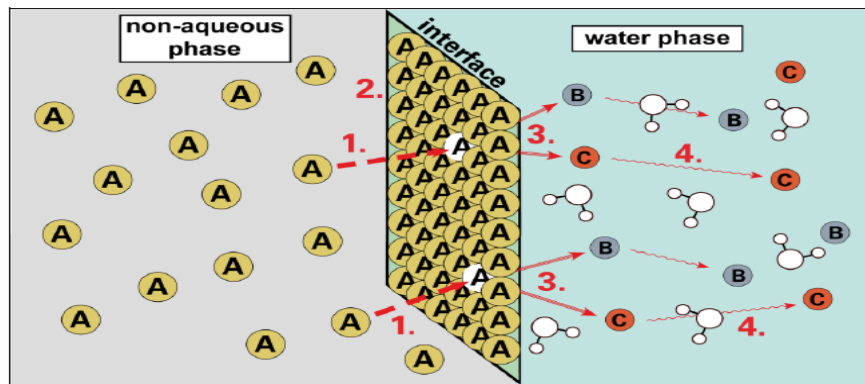
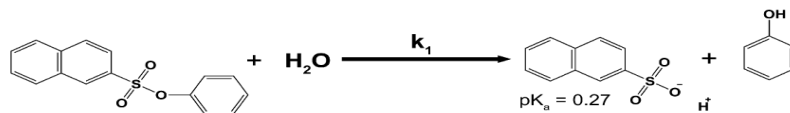
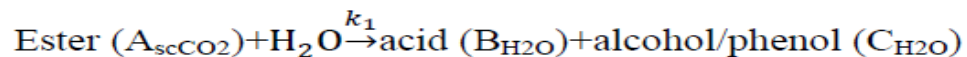


Fig. 2 Schematic representation of all involved processes at the scCO₂/water interface during KIS tracer application, Schaffer et al. 2013.



Phenyl naphthalene-2-sulfonate (2-NSAPh)

Naphthalene - 2-sulfonic acid (2NSA)

Phenol

Objectives

- 1) to develop a novel numerical model to simulate the KIS tracer reaction & transport process in the two-phase flow system based on the lab experiment;
- 2) to evaluate the development of the specific interfacial area between the two phases during the injection of non-wetting phase.

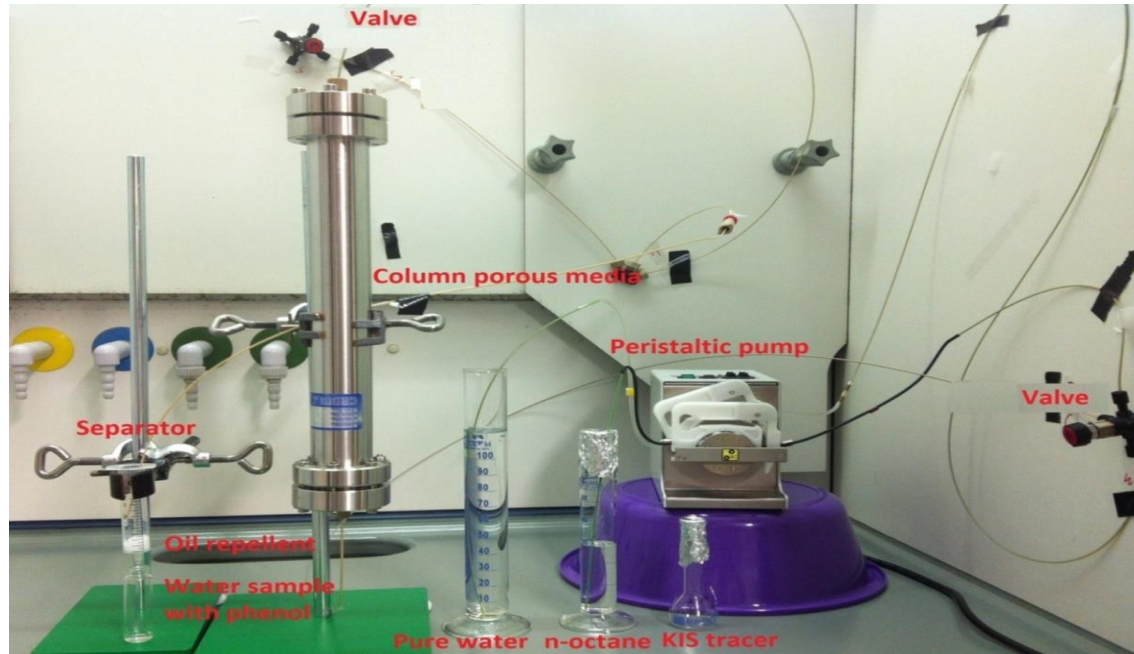


Fig. 3 Experiment set-up

Non-wetting phase: n-octane
Wetting phase: water

Numerical modeling

- 1) Two-phase flow - pressure-saturation formulation (Helmig, 1997).

$$L_{\alpha}(p_{\alpha}, S_{\alpha}) := \phi \varrho_{\alpha} \frac{\partial S_{\alpha}}{\partial t} + \varrho_{\alpha} S_{\alpha} \frac{\partial \phi}{\partial t} + \phi S_{\alpha} \frac{\partial \varrho}{\partial p} \frac{\partial p}{\partial t} - \nabla \cdot \left\{ \varrho_{\alpha} \frac{k_{r\alpha}}{\mu_{\alpha}} \mathbf{k} \cdot (\mathbf{grad} p_{\alpha} - \varrho_{\alpha} \mathbf{g}) - \varrho_{\alpha} \mathbf{q}_{\alpha} \right\} = 0$$

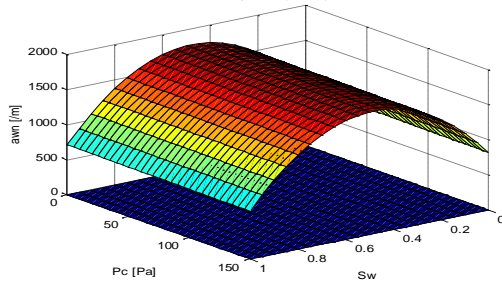
- 2) Reactive tracer transport- mass transfer (Helmig, 1997)

$$L(v_{\alpha}, X_{\alpha}^i) := \int_G \left[\frac{\partial(\phi S_{\alpha} \varrho_{\alpha} X_{\alpha}^i)}{\partial t} + \nabla \cdot \{ \varrho_{\alpha} \mathbf{v}_{\alpha} X_{\alpha}^i - \phi S_{\alpha} \mathbf{D}_{pm,\alpha}^i \cdot (\varrho_{\alpha} \mathbf{grad} X_{\alpha}^i) - r_{\alpha}^i \} \right] dG = 0$$

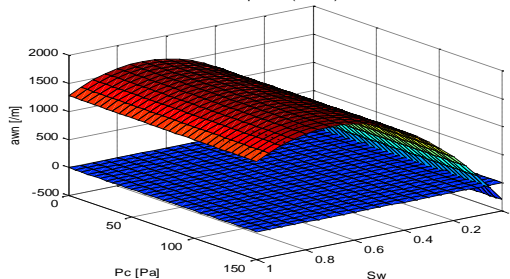
- 3) Specific interfacial area (Hassanizadeh, 1990; Niasar et al, 2010; Niessner, 2008)

$$a_{wn} = \frac{A}{V}$$

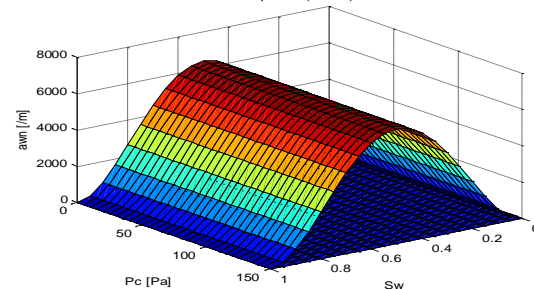
Equation (2.21 a)



Equation (2.21 b)



Equation (2.22 a)



$$a_{\alpha\beta}(S_w, p_c) = 849 + 3858S_w - 0.224p_c + 0.006S_w p_c - 39925S_w^2 - 39925S_w^2 + 1.283(e-5)p_c^2$$

$$a_{\alpha\beta}(S_w, p_c) = -313.6 + 5535S_w + 0.085p_c - 0.307S_w p_c - 39375S_w^2 - 39375S_w^2 - 5(e-6)p_c^2$$

$$a_{\alpha\beta}(S_w, p_c) = 1 \cdot (S_w)^2 \cdot (1 - S_w)^2 (15000 - p_c)^{1.2}$$

Fig. 4 The p_c - S_w - a_{wn} relationship

Numerical modeling

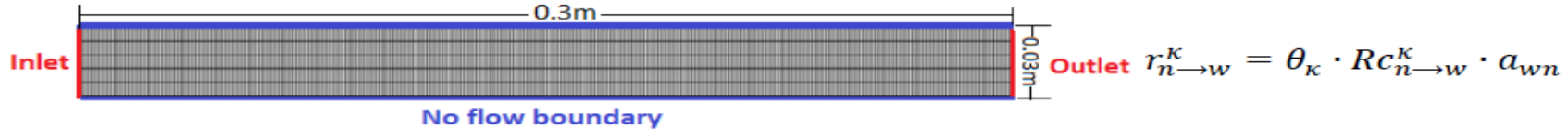


Fig.5 Boundary conditions

Two phase flow model

Pressure-saturation equation

$$\begin{bmatrix} 0 & -\phi \cdot \rho_w \\ 0 & \phi \cdot \rho_n \end{bmatrix} \cdot \begin{bmatrix} \frac{\partial p_w}{\partial t} \\ \frac{\partial S_n}{\partial t} \end{bmatrix} = \nabla \cdot \begin{bmatrix} k \cdot \rho \cdot k_{rw} / \mu_w & 0 \\ k_Q k_{rn} / \mu_n & k_Q k_{rn} / \mu_n \cdot \frac{dp_c}{dS_n} \end{bmatrix} \cdot \nabla \cdot \begin{bmatrix} p_w \\ S_n \end{bmatrix}$$

$$\frac{dp_c}{dS_n} = \frac{1}{\lambda} \cdot p_d \cdot \left(\frac{1-S_n-S_{wr}}{1-S_{wr}} \right)^{(-\frac{1}{\lambda}-1)}$$

Inlet - Neumann boundary condition

$$\nabla \cdot \begin{bmatrix} k \cdot \rho \cdot k_{rw} / \mu & 0 \\ k_Q k_{rn} / \mu & k_Q k_{rn} / \mu \cdot p_c'(S_n) \end{bmatrix}_{x=0} \cdot \nabla \cdot \begin{bmatrix} p_w \\ S_n \end{bmatrix}_{x=0} = \begin{bmatrix} 0 \\ q \end{bmatrix}$$

Outlet - Dirichlet boundary condition

$$\begin{bmatrix} p_w \\ S_n \end{bmatrix}_{x=0.3m} = \begin{bmatrix} p_{w_outlet} \\ S_{n_outlet} \end{bmatrix}$$

No flow - Neumann boundary condition

$$\nabla \cdot \begin{bmatrix} k \cdot \rho \cdot k_{rw} / \mu & 0 \\ k_Q k_{rn} / \mu & k_Q k_{rn} / \mu \cdot p_c'(S_n) \end{bmatrix}_{y=0 \& 0.03m} \cdot \nabla \cdot \begin{bmatrix} p_w \\ S_n \end{bmatrix}_{y=0 \& 0.03m} = 0$$

Solute transport model

Mass transport equation

$$\begin{cases} \phi S_n \frac{\partial c_i}{\partial t} + \phi c_i \frac{\partial S_n}{\partial t} + \nabla \cdot (c_i \mathbf{v}_i) - \nabla \cdot [(D_{dis,i} + D_{dif,i}) \nabla c_i] = -r_i \\ \phi S_w \frac{\partial c_j}{\partial t} + \phi c_j \frac{\partial S_w}{\partial t} + \nabla \cdot (c_j \mathbf{v}_j) - \nabla \cdot [(D_{dis,j} + D_{dif,j}) \nabla c_j] = r_j \end{cases}$$

Inlet - Dirichlet boundary condition

$$\begin{bmatrix} c_i \\ c_j \end{bmatrix}_{x=0} = \begin{bmatrix} c_{in} \\ 0 \end{bmatrix}$$

Outlet - Neumann boundary condition

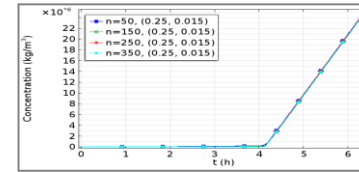
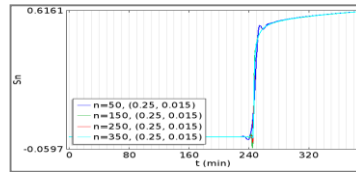
$$-\nabla \cdot \begin{bmatrix} (D_{dis,i} + D_{dif,i}) \nabla c_i \\ (D_{dis,j} + D_{dif,j}) \nabla c_j \end{bmatrix}_{x=0.3m} = 0$$

No flow - Neumann boundary condition

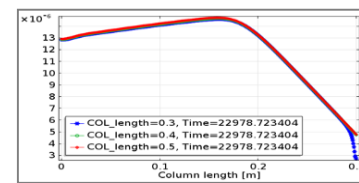
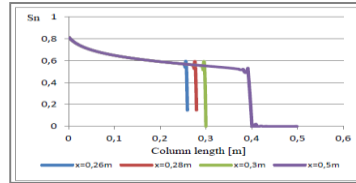
$$-\nabla \cdot \begin{bmatrix} (D_{dis,i} + D_{dif,i}) \nabla c_i \\ (D_{dis,j} + D_{dif,j}) \nabla c_j \end{bmatrix}_{y=0 \& 0.03m} = 0$$

Numerical modeling

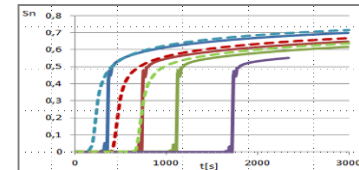
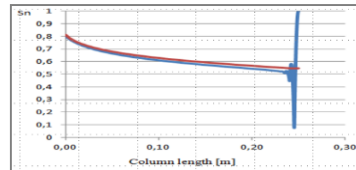
1) Discretization effect



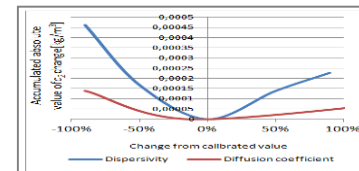
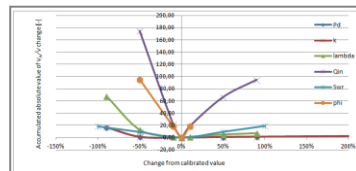
2) Boundary effect



3) Bench marking



4) Sensitivity analysis



Results

1) Breakthrough curves

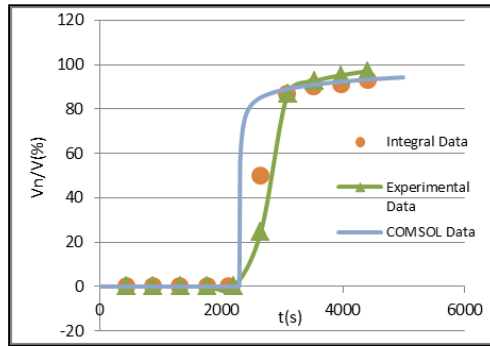
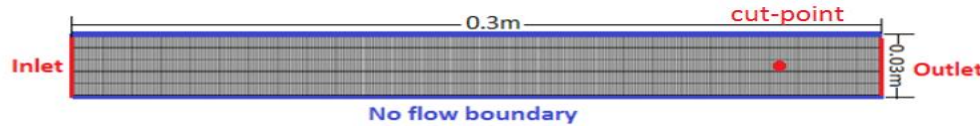


Fig.6 Experimental and simulated breakthrough curves of n-octane ($x=0.25\text{m}$)

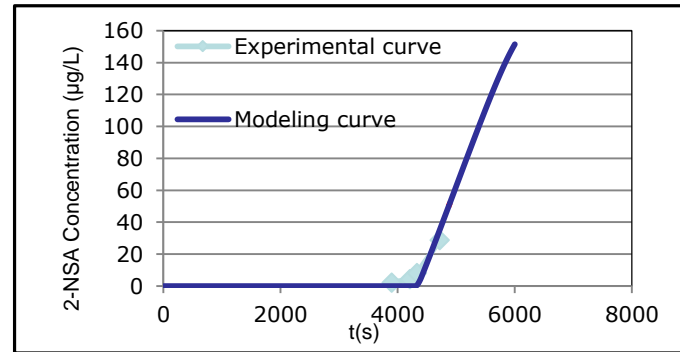


Fig. 7 Experimental and simulated breakthrough curves of 2-NSA ($x=0.25\text{m}$)

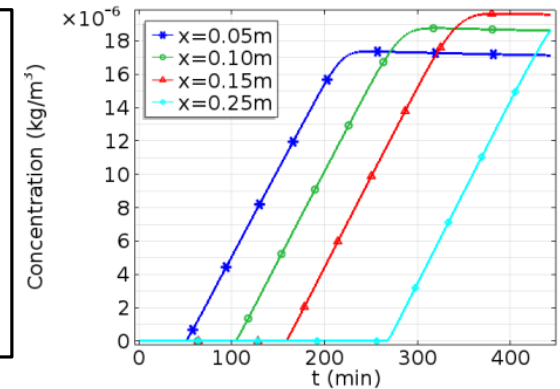


Fig. 8. Breakthrough curve of c_2 at different cut points

2) Relationship between S_n , a_{wn} , C , C_2

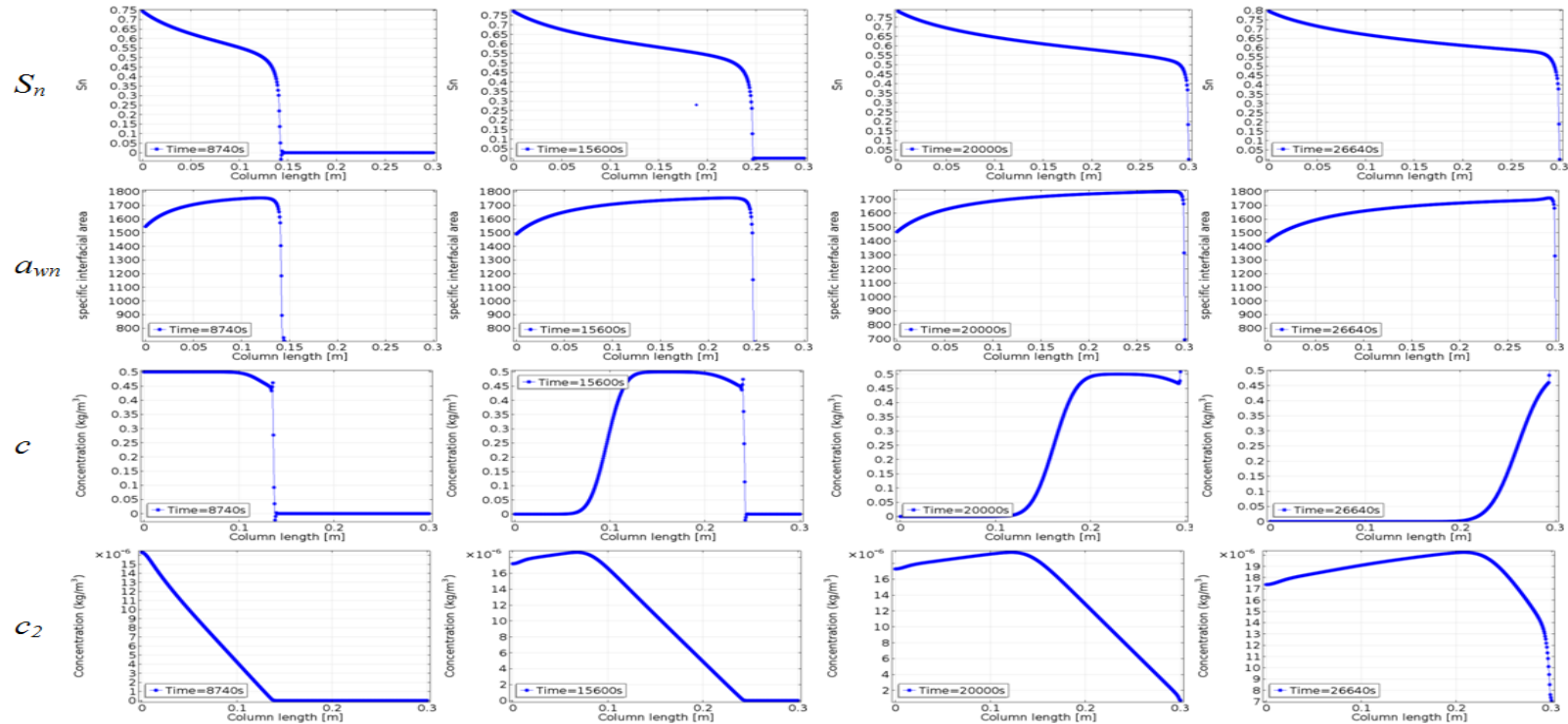


Fig. 8 Breakthrough process of S_n , a_{wn} , c and c_2 along the column porous media at different time step

Conclusion

- 1) The numerical model can be used to simulate the two-phase flow system and tracer reaction and transport processes;
- 2) An average specific interfacial area between the two phases in the column is around 1650/m at the final stage.

References

Hassanizadeh, S. M & Gray, W.G 1990, 'Mechanics and thermodynamics of multi-phase flow in porous media including interphase boundaries', *Advances in Water Resources*, vol. 13, pp. 169–186.

Helmig, R 1997, *Multiphase flow and transport processes in the subsurface: A contribution to the modeling of hydrosystems*, Springer, Berlin, Heidelberg.

Joekar-Niasar, V, Hassanizadeh, S. M & Dahle, H. K 2010, 'Non-equilibrium effects in capillarity and interfacial area in two-phase flow: dynamic pore-network modelling', *Journal of Fluid Mechanics*, vol. 655, pp. 38–71.

Niessner, J & Hassanizadeh, S. M 2008, 'A model for two-phase flow in porous media including fluid-fluid interfacial area', *Water Resources Research*, vol. 44, W08439, doi:10.1029/2007WR006721.

Schaffer, M, Maier, F, Licha, T & Sauter, M 2013, 'A new generation of tracers for the characterization of interfacial areas during supercritical carbon dioxide injections into deep saline aquifers: Kinetic interface sensitive tracers (KIS tracer)', *International Journal of Greenhouse Gas Control*, vol. 14, pp. 200–208.

Thank you for your attention!

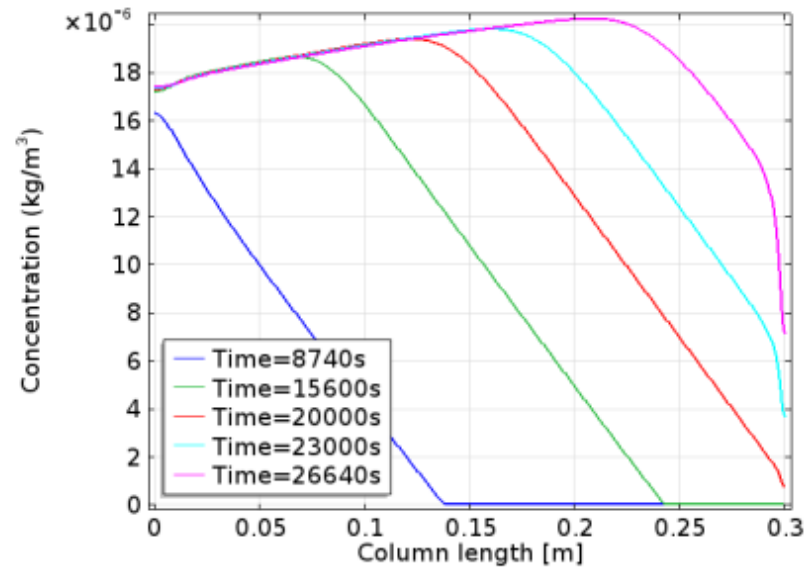


Figure 5. 36 Distribution curves of phenol concentration c_2 at different time point